Analysis of parallel connected lithium-ion cells imbalanced performance based on electrothermal modelling environment

Gabriele Piombo
Warwick Manufacturing Group
University of Warwick
Coventry, United Kingdom
gabriele.piombo@warwick.ac.uk

James Marco
Warwick Manufacturing Group
University of Warwick
Coventry, United Kingdom
james.marco@warwick.ac.uk

Richard Boyd
Altair Engineering (UK), Ltd.
Royal Leamington Spa, United Kingdom
richard.boyd@uk.altair.com

Abstract*—Typical battery management systems (BMS) do not provide the opportunity of monitoring each parallel string cell individually, rather considering cells operate at common voltage and current levels. In reality, manufacturing induced characteristics imbalances, pack thermal gradients and interconnection resistances impose uneven states among cells. As such, this paper intends to take advantage of common Equivalent Circuit Modelling (ECM) approaches to investigate the incurring interrelationships among 15 cells connected in parallel. The module is discharged under real-world drive cycle conditions in different scenarios, aligning model parameters variation to literature based evidence to accurately replicate their impact on imbalanced performance. The simulation results indicate a 1% ratio between interconnection resistance and internal resistance has the largest influence on cell-to-cell load current imbalance and thermal gradient among the investigated factors. Second, manufacturing related 25% internal resistance variability and poor cooling system design induced thermal gradient caused non-negligible imbalances in cells' performance. A 9% cell-to-cell variation of capacity, contrarily, emerged as having a limited impact on pack behaviour, although constant current loads could imply different conclusions. Last, between investigated Z and Ladder pack configurations, the first choice guaranteed a more uniform performance. This work draws attention to the fact that the presence of imbalances not captured by the BMS can have a detrimental impact on the performance of different pack areas. Hence, the developed Activate® ECM pack model will be coupled in future work with HyperStudy® optimization tool to perform sensitivity analysis. This is expected to improve and accelerate the pack design process ensuring diagnostics and prevention of protracting imbalances, lowering pack safety and degradation concerns.

Keywords—Lithium-ion batteries, Parallel connection, Equivalent Circuit Models (ECM), Pack imbalanced performance, Simulation, Interconnection resistance, Thermal gradient, Manufacturing inconsistency

I. INTRODUCTION

The 2015 Paris international treaty on climate change includes long-term plans for the reduction of the level of carbon dioxide and greenhouse gases emissions in the atmosphere across different sectors. In numbers, the emissions of pollutants are required to be reduced by 80% to 95% by 2050 compared to the levels of 1990 [1]. The decarbonisation of the transport sector plays a crucial role in achieving the set milestone of keeping global warming below 1.5°C compared to pre-industrial levels, accounting for 23% of global carbon dioxide emissions [2]. Different solutions were researched over the last decades to offer alternatives to conventionally fuelled vehicles, with macro-areas including alternative fuels, hydrogen and electrochemical storage [3]. The automotive industry sector trend appeared to be uniform, identifying Lithium-ion batteries as the ideal solution for vehicle implementation. High specific energy, a large number of charge-discharge cycles and year-on-year reducing cost [4] represent the desired properties to match the wide range of requirements typical of vehicle application [5].

In an automotive system, single cells are not suitable to guarantee, individually, the voltage and energy contents characteristics required by their application. To minimize conductors size and losses low current levels must be maintained. Hence, a voltage higher than the nominal one has to be achieved by arranging individual cells in series. On the other hand, to ensure adequate energy capacity values ensuring desired range achievement, cells are arranged in parallel [6]. The combination of the series and parallel connected cells in different numbers composes the modules. Modules are then assembled into the whole battery pack, which is commonly composed of hundreds to thousands of cells. The coexistence of multiple cells in the same system introduces interdependencies among them, resulting in different degradation rates when compared to individual cells, even though correlated [7]. Ideally, when cells are connected in parallel, they share the same terminal voltage. Nevertheless, current imbalance occurs due to different causes as manufacturing inconsistencies, poor pack design or interconnection resistances [8], [9]. The protracted imbalances can induce state of charge (SoC) and state of health (SoH) variations across the pack. The battery management system does not usually offer online monitoring of current imbalances or individual cells' properties due to the otherwise uprising equipment costs and usually assumes cells share the same characteristics [10]. The difference between actual and assumed cell properties can exacerbate the pack condition, accelerating degradation and increasing safety concerns [11].

Despite the literature offers a wide investigation of cell behaviour, from chemistry analysis to electrochemical characterization, the theme of parallel connection of cells leaves empty spaces in the knowledge and requires further research [12], [13]. Particularly, parallel connection induced load current imbalance, over-time internal resistance, capacity, SoC and SoH cell-to-cell variation are among the subjects requiring further investigation. Increasing the level of understanding of these topics means being able to better diagnose and prognoses the whole pack conditions, potentially

improving their safety, performance and ageing. Coherently, this paper aims to analyse the factors influencing the imbalanced performance of battery packs due to the connection of cells in parallel through electrothermal modelling techniques.

The structure of this work is divided as follows: Section 2 explains the modelling approach pursued. There, the mathematical formulation of the electrical and thermal models is offered together with their software implementation. Section 3 introduces the validation process and the boundary conditions for model applicability. The simulation setup and results are given in Section 4, where the pack performance imbalance influencing factors are analysed. Last, Section 6 summarises the conclusions and limitations of this study and presents emerging further work opportunities.

II. MODEL FRAMEWORK

A. *Electrical model*

The models and simulations were developed using Altair's Activate tool, which is a multi-domain system simulation software based on a hybrid block diagram modelling environment. The tool is suitable to simulate multi-physics at a system level by including electric, thermal and object-oriented physical components together with different scripting languages in a single framework like the one included in Fig. 1. The advantage of an object-oriented approach includes the availability of a structured and unified representation allowing the management of the information and physics of components in a system environment. Activate added value resides in the possibility of co-simulating with other Altair tools. Among them, Hyperstudy allows design of experiments and sensitivity analysis setup and will be next linked with Activate to perform system-level optimisation. Within the literature, previous studies were published on the topic of parallel connection of cells. Nevertheless, to the knowledge of the author, this is the first example based on Activate software. Wang et al. [14] and Zhang et al. [15] founded their simulations on Mathwork's Simscape, while Gong et al. [16] on Simulink. All the three approaches lack a deep analysis of the current distribution over the parallel cells, mainly due to neglecting the contact resistance hence levelling cell-to-cell variation. Other studies [17] offered the inclusion of the contact resistance in the simulation and captured its impact on the performance of the system. Nevertheless, the simulations were based on electrochemical models, less suitable for highly parallelised systems.

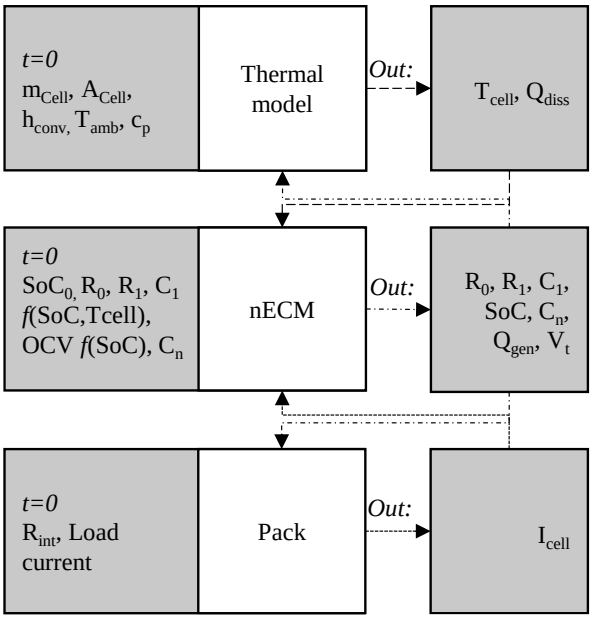

Fig. 1 System model framework

In this study, a parallel string "lumped" model was developed. Commonly, the parameters of individual cells are scaled to form a parallel unit, following the same mathematical formulation of single cells. This approach is suitable for new cells, where neglecting manufacturing inconsistencies it can be assumed cells share the same characteristics. Nevertheless, there is no certainty around the fact that cells will degrade evenly, especially when connected in parallel [18]. Coherently, the developed model takes into consideration the characteristics of individual cells, by including both electrical and thermal models for each of them. In this way, it is possible to capture the interrelationships occurring among the cells by considering they do not undergo the same electrical and thermal loading. Current imbalances, SoC divergence, temperature gradients are examples of the phenomena that this approach allows to consider.

The mathematical formulation of the electrical and thermal models is offered here below. The ECM technique was selected as it represents a good compromise between accuracy and computational effort [19], [20]. The ECM is commonly adopted to replicate the voltage response of individual cells. It is relatively simple, easy to parametrise and offers the possibility of real-time simulations [20], [21]. ECMs do not replicate the electrochemical physics occurring inside the cell, simply matching the voltage response on the current input. Nevertheless, the elements of the circuit presented in Fig. 2 offer the chance of being linked back to physical aspects as charge transfer and diffusion [10]. In Fig. 2 and Fig. 3 the schematic of the model is presented, by

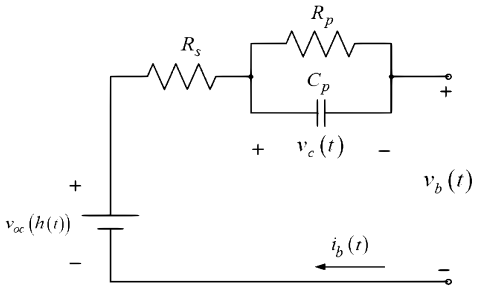

Fig. 2 Sketch of an individual cell ECM [22]

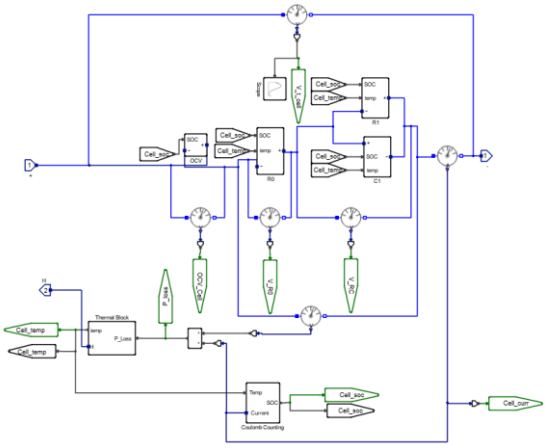

Fig. 3 Activate blocks single cell ECM representation

comparing the sketch and the actual Activate block representation respectively.

$$V_t(t) = V_{OCV} - V_p(t) + R_0 * I(t) \quad (1)$$

$$d(V_p(t))/dt = -(V_p(t))/(C_1 * R_1) + I(t)/C_1 \quad (2)$$

$$d(SOC)/dt = \eta/Q_{RATED} * I(t) \quad (3)$$

R_0, R_P and C_P represent the internal resistance and the polarization resistance and capacitor respectively. V_{OCV} indicates the open-circuit voltage (OCV).

Each of the circuit elements is a sub-system including Activate software specific electrical blocks. The values of the parameters in each block are included as lookup tables in their Activate implementation. Specifically, resistances and capacity are function of SoC and temperature, while open circuit voltage is function of SoC. The software independently calculates and displays the voltage response, current and SoC of each cell upon (1), (2), (3) in real-time. The calculated state of charge is fed back to the open-circuit voltage as a lookup table variable. The choice of the ECM approach implies that the model needs to undergo parameters characterisation first, whose reference test is the "Hybrid Pulse Power Characterization" (HPPC) test. The experiment outcomes can be directly fed as lookup tables in the model blocks.

B. Thermal model

Each ECM includes a thermal model, which can calculate based upon the cells' heat generation and dissipation the temperature increase/decrease. The cell temperature is then fed back to the ECM electrical blocks to allow their calculation upon lookup tables. The thermal model considers the dissipation to the ambient only. The inclusion of a cooling system is left out of the scope of this work, being understanding parallel cells' interrelationships. Nevertheless, it can be made available following the same procedure as for ambient. In Fig. 4, the Activate block representation of the thermal model is included. The mathematical foundation of the thermal system can be exposed by referring to the energy balance equation:

$$dE/dt = m*C_p*dT/dt = Q_{Gen} - Q_{Diss} \quad (4)$$

$$Q_{Gen} = I(t)*(U(t)-U_{OCV}) + I(t)*T*dU_{OCV}/dT \quad (5)$$

$$Q_{Diss} = 1/R_{Amb}*(T_{Cell}-T_{Amb}) \quad (6)$$

$$R_{Convective} = 1/hA = \Delta x/(Nu*k)*A \quad (7)$$

Where:

dE/dt: Rate of change in system energy over time, [J/s]

m : Module mass, [kg]

C_p : Module heat capacity, usually a function of temperature, [J/kg*K]

dT/dt: Cooling/heating rate, [K/s]

Q_{Gen} : Module heat generation rate, [W]

Q_{Diss} : Module heat rejection rate or heat losses, [W]

$R_{Convective}$: Thermal resistance for convection [K/W]

Δx : Thickness of the layer [m]

k : Thermal conductivity [W/mK]

h : Convective heat transfer coefficient [W/m^{2}K]

Nu : Dimensionless Nusselt number

A : Cross sectional area [m^2]

The single cell model described up to this point can be extended to parallel strings by connecting different ECMs. Activate software offers the possibility of automatically linking the blocks taking advantage of its multi-physics capabilities, being able to consider both electrical and thermal blocks simultaneously. In this work, a 15 cells parallel string is investigated, although the same methodology is valid for n-cells. Interconnection resistances are included between cells, as it emerged from the literature study being one of the main contributors to current load imbalance. The resulting system is included in Fig. 5. The initialisation setup is done through a "Model" script developed in Altair Compose® language, run at the first simulation step. The initialisation parameters include the ECM parameters as a function of their respective variables forming the lookup tables, initial ambient and cell temperature, SoC, cell geometric dimensions, convective heat transfer coefficient, thermal capacity, drive cycle load current, simulation duration and time step.

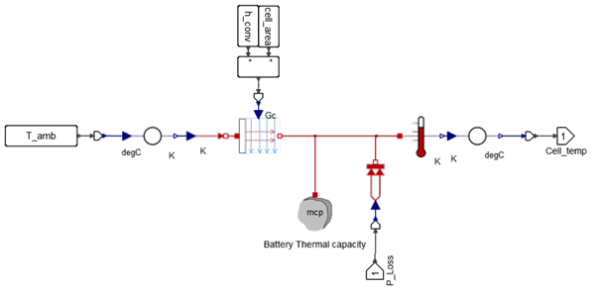

Fig. 4 Thermal model Activate block representation

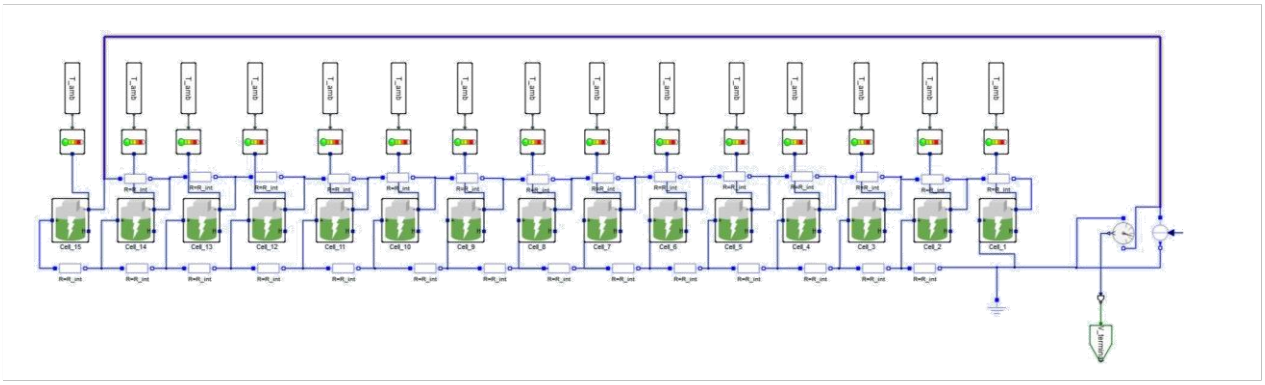

Fig. 5 15P string Activate block representation (Z)

III. MODEL VALIDATION

A. Single cell level

The parameters characterisation of the cells has been carried out based upon data previously published by Hosseinzadeh et al. [23]. Hence, the validation procedure has been maintained consistent with the one adopted in [23]. Experimental data gathered at 25°C ambient temperature cycling the cell under a predefined current load presented were used as the baseline. The single cell model is validated upon terminal voltage and surface temperature. The temperature measurement was collected at cells' middle surface through T type thermocouples. The single cell model simulation results show good alignment with the experimental data. The peak terminal voltage error is in the order of 0.1 V, coherent with the values reported in [23], while the root mean square (RMS) error is 0.04 V against 0.08 V. The surface temperature deviates from experimental data of 1.2°C peak and 0.4°C RMS, slightly larger values than the maximum deviation of 1°C obtained in [23].

B. Module level

The module level validation was carried out by coupling 4 single cells ECMs in parallel in a ladder configuration. Coherently with Hosseinzadeh article, the validation was done by comparing simulation results to published data included in Bruen work [10]. To validate the model response to unbalances, the four cells parameters were set to differ in terms of initial capacity and internal resistance, whose values are available in Table 3 in [23]. This differentiation is considered representative of different SoH conditions of the single cells, aged by 0, 50, 100 and 150 cycles respectively. The interconnection resistance impact over experimental results has been neglected due to the setup, connecting wires from each cell to a common pair of terminals. The simulation results showed a terminal voltage peak error of 0.13 V and a RMS error of 0.05 V. The current imbalance among the cells was accurately captured by the model with a 0.4 A peak error and RMS errors between 0.02 A and 0.04 A for the four cells. Comparing the developed model simulation results to Hosseinzadeh model, the validation parameters showed similar RMS error orders of magnitude for terminal voltage, current and temperature.

IV. RESULTS AND DISCUSSION

A. Simulation setup

Increasing the level of understanding of design parameters impact on pack performance unevenness in parallel connected cells plays an important role in increasing battery safety. Over/under-charge/discharge and temperature gradients are among phenomena requiring to be limited. Besides, precisely estimating cells behaviour is crucial when addressing control strategies aimed to minimize cells degradation. On that intent, the creation of an ECM model is aimed to have a validated tool with estimation capabilities.

The load profile applied to the string was obtained from a real-world instrumented car and is presented in Fig. 6. Being real-world derived, it represents a good approximation of a potential driver vehicle usage in a mild urban/highway scenario. The case studies include discharge from 90% to 5% SoC. After cycling, cells are left the time to self-balance. Environmental conditions are kept coherent with validated boundaries and set to be 25°C.

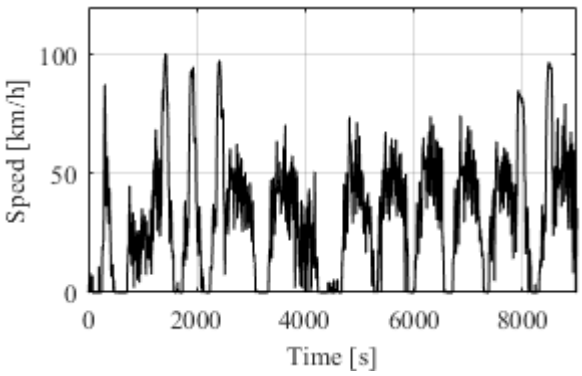

Fig. 6 Drive cycle speed profile

To systematically identify the level of states variation caused by the evaluated scenarios, different parameters are introduced. First, the state mean and standard deviation in their conventional form, which will be applied to current and SoC to evaluate their dispersion at different depth of discharge.

$$\mu = (1/N)\,\Sigma\, x_i \tag{8}$$

$$\sigma = \sqrt{[\,\Sigma\,(x_i-\mu)^2/(N-1)]} \tag{9}$$

Second, the "Time To Discharge" (TTD) targets understanding the variations in discharge duration and hence how far in the drive cycle the battery can last. Third, the "Time To Self-Balance" (TTSB), is introduced to identify how far do the imbalances protract once the cycle ends. The end of equilibration is considered once the driven current reaches 1mA.

B. Interconnection resistance

Among the possible ways of connecting cells in parallel, the most diffused ones are Z and Ladder configurations [7]. The differentiation of the two configurations aims to estimate the differences inherent the two approaches and giving insights on the outcomes of either the choices in the design phase. The comparison between Z and Ladder approaches is based upon the impact that interconnection resistance has on the current imbalance. Specifically, understanding that the R_{IC} is in the order of 1% to 10% of R_0 [24], values of 19.3e-2 mΩ to 19.3e-1 mΩ are included in the model among each cell. The remaining parameters, namely initial capacity, resistance, SoC, initial temperature and thermal boundaries are imposed as equal among the cells.

1) Z configuration: As it can be noticed from Activate representation in Fig. 5, when connected in Z configuration, the pack shows symmetry around the middle cell/s. This intrinsically induces cells at the extremities (1 and 15) to have mirrored behaviour (assuming no further variations). As they show the lowest resistance in the pack, they carry the highest current and vice versa. This protracted imbalance induces a condition where at the moment cells 1 and 15 approximately reach 5% SoC, being the end of the cycle, cell 8 shows a higher SoC. The unevenness of charge states at the end of the cycle causes an equilibration period of 2586s. The current variation in the pack correlates with the temperature spread, which reaches a maximum of 2.2°C over the cycle. The tabularized simulation results can be found in Table I.

2) Ladder configuration: Connecting the 15 cells in parallel following a Ladder approach induces a side of the pack, namely the one closer to the terminal, to face the highest currents. This is related to the fact that the amount of resistance they face is the lowest. This translates in cell 15 experiencing the lowest current of the pack against cell 1 acting oppositely. The lack of symmetry Ladder configuration shows influences the level of unevenness experienced by the pack, resulting in a maximum current deviation circa 220% higher than in the case of Z connection. Temperature gradient coherently achieves large values, namely 9.1°C over the cycle. Combined, these factors induce the final state of charge to be different between the first and last cell, ending at 5% and 17.1% respectively. The equilibration period results then incremented to 3984s.

In general, the Ladder approach shows the highest variations in terms of voltage, current and temperature among the cells of the pack, reducing the TTD to 5685s against 6196s of Z configuration. This raises concerns over the long term impacts of protracting large imbalances in the behaviour of single cells, although not investigated in this report. In the short-term, the level of unevenness both the configurations achieve shows managing the cells properly is crucial to protect against over/under-charging/discharging and temperature induced failures. Lower criticality is presented by the Z approach, whose symmetry appears to guarantee lower imbalances than the Ladder approach.

C. Thermal gradient

Avoiding temperature peaks ensures safety during operation, while uniform pack temperature, ideally in the order of 5°C, reduces the long term degradation of the cells [25], [26]. To safeguard cells' lifetime, it is therefore necessary to reduce as much as possible not only the peak temperature but also the temperature differences in the pack [27]. Additionally, the cells' internal resistance is known to be inversely proportional to temperature [28], impacting in-cycle current distribution and introducing positive temperature feedback [23]. The reasons for uneven temperature distribution in the pack can be found in poor cooling system design, poor contact between the cell and the cooling plate or decay in the thermal pad [5], [25]. To understand and evaluate the impact the temperature has on parallel cells' behaviour, a temperature gradient is forced in the pack. On that intent, cells' 1-3 heat transfer coefficient is set to 0 [W/m^{2}K] to simulate their full insulation.

In the absence of interconnection resistance cells behave uniformly both in Z and Ladder arrangements. For simplicity, only the simulation results obtained for the Ladder configuration are reported from this point onward. Cells 4-15 show similar behaviour trends, while cells 1-3 vary majorly. Current, particularly, results largely driven towards the insulated cells. The higher temperature reached by cells 1-3 lowers the internal resistance, increasing further the driven current and leading σ_I to 1.1A. In turn, σ_{SoC} increases to 0.6%, meaning the pack could not release its full energy potential. The temperature gradient in the pack reaches a maximum of 23.9°C. The TTD and TTSB are 6198s and 2566s respectively, as reported in Fig. 7.

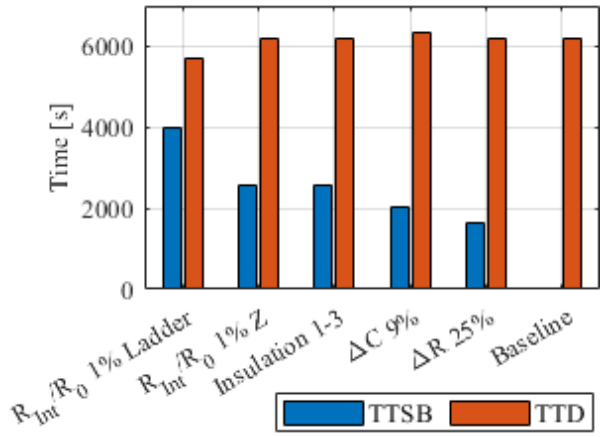

Fig. 7 Different scenarios simulated TTSB and TTD bar chart

Lowering cells internal resistance due to higher temperatures means they will drive more current. In line with the results obtained in the previous section, a pack can show areas where imbalances concentration is higher. These are closer to the terminal both for Ladder and Z configuration in real conditions. Hence, a poor cooling design induced temperature increase in these areas could mean an exacerbation of the current imbalance. Contrarily, if the insulation happens in the cells' furthest from terminals, the current imbalance would be reduced to the detriment of temperature uniformity.

D. Manufacturing inconsistency

The differences between the design phase outcomes and the actual production results are dependent, among other factors, on the accuracy of the manufacturing process. When manufacturing complex systems as the battery pack, it is therefore to be considered a potential level of variation introduced by the nature of the process. Manufacture related cell-to-cell variations in terms of capacity and internal resistance are addressed in this section to evaluate their impact on pack imbalances.

1) Capacity variation: Capacity cell-to-cell variation is known to have a detrimental impact on the total capacity of a parallel-connected string [14], [29]. In the case where two cells are connected in parallel and they differ in terms of capacity, whilst sharing equal remaining characteristics, they

TABLE I. SIMULATION RESULTS SUMMARY

Specificity	Configuration	σ_I [A]	μ_I [A]	σ_{SoC} [%]	μ_{SoC} [%]	ΔT_{max} [°C]	TTSB [s]	TTD [s]
Baseline	Z/Ladder	0.0	16.2	0.0	5.0	0.0	0.0	6215
R_{int}/R_0=1%	Z	2.4	16.2	0.8	6.3	2.2	2586	6196
R_{int}/R_0=1%	Ladder	7.5	16.2	4.0	12.5	9.1	3984	5685
HTC_{1-3}=0 [W/m^{2}K]	Z/Ladder	1.1	17.3	0.6	6.2	23.4	2567	6198
ΔR_0=25%	Z/Ladder	1.3	16.2	0.4	5.8	0.4	1647	6204
ΔC=9%	Z/Ladder	0.4	12.1	0.4	5.8	0.8	2040	6338

will undergo different loads when cycled. After the first time step sharing the same SoC, the cell with the higher capacity will reach higher SoC than the other cell in case of discharge and lower SoC in case of charge. In real-world conditions, the dependency of the internal resistance on the SoC of the cell can not be disregarded, especially at low SoC values and for certain chemistries, as it influences directly the load the cell will undergo [30]. Nevertheless, just in this logic chain the variation of RCELL on SoC is not considered to isolate capacity contribution. It follows that to counterbalance the lower (discharge) or higher (charge) SoC level reached by the lower capacity cell, it will always undergo the lowest current load of the two cells. This is directly connected to the open-circuit voltage, which is a function of the SoC. In this case study, a literature reference value of 9% for manufacturing inconsistency related capacity [30], [31] is first imposed, whose outcomes are reported in Table I.

It has to be pointed out that a random allocation of capacity variability was performed, leading cells 1 and 15 to have the highest and lowest values of capacity respectively. Coherently, they show the highest and lowest current load. Capacity influence on pack degree of unevenness develops over time, consistently with SoC deviation. Current imbalance, in particular, although being limited when compared to other scenarios, shows an increase over the drive cycle. As a result, a maximum σ_I of 0.4A occurs towards the end of cycle and leads σ_I to reach 0.4%. The following equilibration period lasts 2040s. The averagely higher nominal capacity of this scenario induced the TTD to reach 6338s.

A previous study concluded that even in the case of a large capacity variation, the current imbalance generated is lower than the one caused by internal resistance cell-to-cell variation, assuming the same orders of magnitude of values oscillation [32].

2) Resistance variation: When connecting multiple cells in parallel, the current divider equation applies [12]. Coherently, the cells having a higher resistance will end up having the lowest current load and vice versa. As pointed out previously, internal resistance is a function of SoC and temperature, other than the cell's chemistry. This dependency leads to varying behaviour of the cells both over the duration and the nature of charging and discharging phases. If cells differ in terms of internal resistance, it can then happen that over-charge/discharge occurs. A 25% resistance variation is resulting from literature as an indication for manufacturing inconsistencies [33] and is coherently taken as reference for this case study. The random allocation of cells resistances leads cells 5 and 8 to have the highest and lowest internal resistances respectively.

In cycle first phases, the current loads spread over the pack following the aforementioned current divider equation. Subsequently, the loads' balance in the central phase diverges again towards the end of the cycle and hence low SoC, where it is acknowledged resistance steeply increases [15]. Contrarily to capacity variation impact, internal resistance causes unevenness in current loads over the whole drive cycle, leading σ_I to 1.3A and σ_{SoC} to 0.4%. The effect of internal resistance has on cell-to-cell current imbalance can not be disregarded.

When comparing the different scenarios discharge profiles, it can be noticed how the influencing factors impact pack performance. In Fig. 8 the SoC profiles of the most discharged cell for each scenario is reported. It emerges the interconnection resistance presence in a ladder configuration leads to an early discharge followed by a long equilibration period. The capacity variation scenario shows a slower SoC descent due to the averagely larger pack nominal capacity. The remaining scenarios show a closer behaviour. Nevertheless, non-negligible SoC deviations occur, as depicted in Fig. 9. The centred probability density functions (PDFs) obtained at end of cycle (EoC) for SoC and at maximum deviation for current show how spread can the states be across the whole cycling. An order of influence can be deducted from this type of representation. Interconnection resistance, thermal gradient and manufacturing inconsistency emerge as having decreasing influence over states spread.

V. CONCLUSIONS AND OUTLOOK

This work targeted achieving a model-based analysis of the performance imbalances caused by interconnection resistance, thermal gradients and manufacturing inconsistency on highly parallelised strings. Different results emerged from

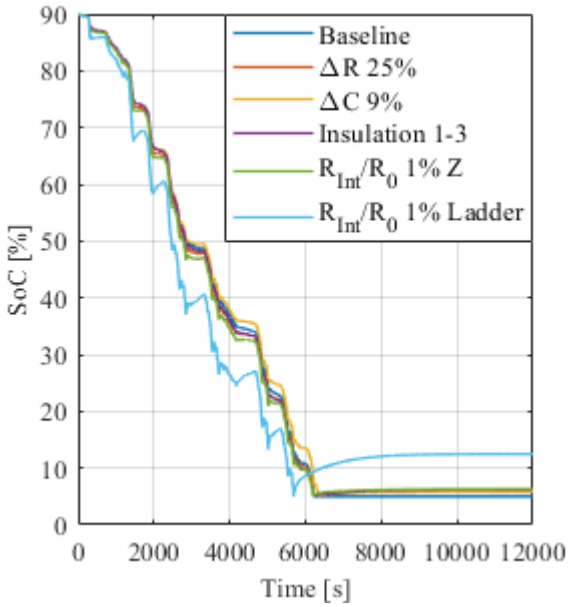

Fig. 8 Investigated scenarios minimum cells' SoC profile

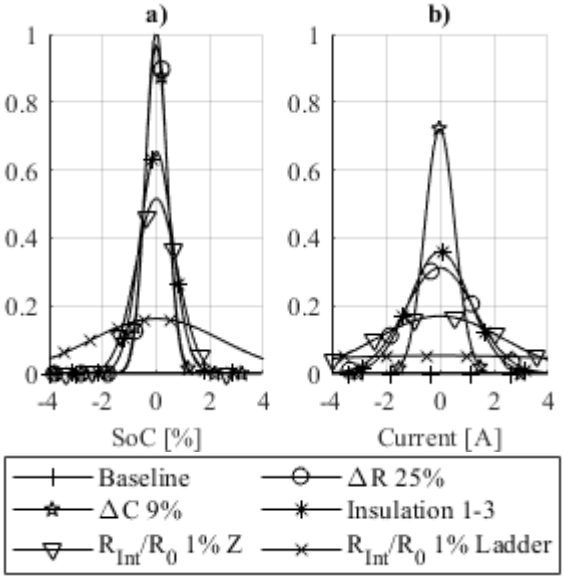

Fig. 9 SoC (a) and Current (b) centered probability density functions

the scenario simulations carried out in this work. First, an order of influence over the pack imbalances can be derived based upon the investigated scenarios. Interconnection resistance showed to have the largest effect over pack behaviour, followed by thermal gradient and internal resistance. Last and less influent, although not negligible especially in the case of constant current loads, capacity variation. Generally, the Ladder configuration resulted in inducing a higher level of unevenness when compared to the Z approach. This is mainly attributable to the symmetry around the central cell/s Z configuration presents, inducing a more even resistance distribution. Coherently, the maximum current difference in the pack will be mitigated by the configuration chosen in the design phase. To conclude, the objectives of this work not only included imbalanced performance analysis but also developing an adequate tool upon which future parameters selection optimisation studies will be established. These studies will be enabled by the suitability of Activate and Hyperstudy co-simulation, offering built-in sensitivity analysis and optimisation capabilities.

ACKNOWLEDGMENT

The research presented within this paper is supported by Altair Engineering (UK) Limited through the Engineering Centre for Doctoral Training in Sustainable Materials and Manufacturing. The authors would like to thank Dr Hosseinzadeh E. and Dr Truong B. (Warwick Manufacturing Group) for providing the model parametrisation and drive cycle datasets. The authors would like to thank also Dr Soulard J. (Warwick Manufacturing Group) for the comments on the manuscript.

REFERENCES

[1] "Towards an Integrated Strategic Energy Technology (SET) Plan: Accelerating the European Energy System Transformation," 2015.

[2] Z. Liu, L. Li, and Y. J. Zhang, "Investigating the CO2 emission differences among China's transport sectors and their influencing factors," Nat. Hazards, vol. 77, no. 2, pp. 1323–1343, Jun. 2015

[3] S. Michaelides, "Alternative Energy Sources" in Springer science & business media, vol. 20, 2012.

[4] B. Kennedy, D. Patterson, and S. Camilleri, "Use of lithium-ion batteries in electric vehicles," J. Power Sources, vol. 90, no. 2, pp. 156–162, Oct. 2000

[5] Q. Wang, B. Jiang, B. Li, and Y. Yan, "A critical review of thermal management models and solutions of lithium-ion batteries for the development of pure electric vehicles," Renewable and Sustainable Energy Reviews, vol. 64. Elsevier Ltd, pp. 106–128, 01-Oct-2016

[6] F. Baronti, R. Di Rienzo, N. Papazafiropulos, R. Roncella, & R. Saletti, "Investigation of series-parallel connections of multi-module batteries for electrified vehicles", in 2014 IEEE (IEVC) (pp. 1-7).

[7] X. Wang, Z. Wang, L. Wang, Z. Wang, and H. Guo, "Dependency analysis and degradation process-dependent modeling of lithium-ion battery packs," J. Power Sources, vol. 414, pp. 318–326, Feb. 2019.

[8] M. Dubarry, N. Vuillaume, and B. Y. Liaw, "Origins and accommodation of cell variations in Li-ion battery pack modeling," Int. J. Energy Res., vol. 34, no. 2, pp. 216–231, Feb. 2010.

[9] S. Santhanagopalan and R. E. White, "Quantifying Cell-to-Cell Variations in Lithium Ion Batteries," Int. J. Electrochem., 2012.

[10] T. Bruen and J. Marco, "Modelling and experimental evaluation of parallel connected lithium ion cells for an electric vehicle battery system," J. Power Sources, vol. 310, pp. 91–101, Apr. 2016.

[11] F. A. Lebel, S. Wilke, B. Schweitzer, M. A. Roux, S. Al-Hallaj, and J. P. F. Trovão, "A lithium-ion battery electro-thermal model of parallellized cells," in IEEE Vehicular Technology Conference, 2016.

[12] M. J. Brand, M. H. Hofmann, M. Steinhardt, S. F. Schuster, and A. Jossen, "Current distribution within parallel-connected battery cells," J. Power Sources, vol. 334, pp. 202–212, Dec. 2016.

[13] C. Campestrini, P. Keil, S. F. Schuster, and A. Jossen, "Ageing of lithium-ion battery modules with dissipative balancing compared with single-cell ageing," J. Energy Storage, vol. 6, pp. 142–152, May 2016.

[14] L. Wang, Y. Cheng, and X. Zhao, "A LiFePO4 battery pack capacity estimation approach considering in-parallel cell safety in electric vehicles," Appl. Energy, vol. 142, pp. 293–302, Mar. 2015.

[15] H. Zhang, T. Wang, R. Lu, C. Zhu, and Y. Zhao, "Study on the Impedance Increase Fault of Parallel Connected Batteries Based on Simscape Model Simulation," in 2015 IEEE Vehicle Power and Propulsion Conference, VPPC 2015 - Proceedings, 2015.

[16] X. Gong, R. Xiong, and C. C. Mi, "Study of the Characteristics of Battery Packs in Electric Vehicles With Parallel-Connected Lithium-Ion Battery Cells," IEEE Trans. Ind. Appl., pp. 1872–1879, Mar. 2015.

[17] B. Wu, V. Yufit, M. Marinescu, G. J. Offer, R. F. Martinez-Botas, and N. P. Brandon, "Coupled thermal-electrochemical modelling of uneven heat generation in lithium-ion battery packs," J. Power Sources, vol. 243, pp. 544–554, Dec. 2013.

[18] T. Baumhöfer, M. Brühl, S. Rothgang, and D. U. Sauer, "Production caused variation in capacity aging trend and correlation to initial cell performance," J. Power Sources, vol. 247, pp. 332–338, 2014.

[19] H. He, R. Xiong, H. Guo, and S. Li, "Comparison study on the battery models used for the energy management of batteries in electric vehicles," in Energy Conversion and Management, 2012.

[20] X. Hu, S. Li, and H. Peng, "A comparative study of equivalent circuit models for Li-ion batteries," J. Power Sources, vol. 198, pp. 359–367, Jan. 2012.

[21] A. Seaman, T. S. Dao, and J. McPhee, "A survey of mathematics-based equivalent-circuit and electrochemical battery models for hybrid and electric vehicle simulation," Journal of Power Sources, vol. 256. Elsevier B.V., pp. 410–423, 15-Jun-2014.

[22] D. Mu, J. Jiang, and C. Zhang, "Online semiparametric identification of lithium-ion batteries using the wavelet-based partially linear battery model," Energies, vol. 6, no. 5, pp. 2583–2604, 2013.

[23] E. Hosseinzadeh, S. Arias, M. Krishna, D. Worwood, A. Barai, D. Widanalage, J. Marco, "Quantifying cell-to-cell variations of a parallel battery module for different pack configurations", Applied Energy 2021, 282, 115859.

[24] P. Taheri, S. Hsieh, and M. Bahrami, "Investigating electrical contact resistance losses in lithium-ion battery assemblies for hybrid and electric vehicles," J. Power Sources, vol. 196, no. 15, pp. 6525–6533, Aug. 2011.

[25] H. Liu, Z. Wei, W. He, and J. Zhao, "Thermal issues about Li-ion batteries and recent progress in battery thermal management systems: A review," Energy Conversion and Management, vol. 150. Elsevier Ltd, pp. 304–330, Oct. 2017.

[26] A. Pesaran, "An approach for designing thermal management systems for electric and hybrid vehicle battery packs" 2015. [Online].

[27] N. Yang, X. Zhang, B. Shang, and G. Li, "Unbalanced discharging and aging due to temperature differences among the cells in a lithium-ion battery pack with parallel combination," J. Power Sources, vol. 306, pp. 733–741, Feb. 2016.

[28] A. Barré, B. Deguilhem, S. Grolleau, M. Gérard, F. Suard, and D. Riu, "A review on lithium-ion battery ageing mechanisms and estimations for automotive applications," Journal of Power Sources, vol. 241. Elsevier, pp. 680–689, 01-Nov-2013.

[29] F. An et al., "Cell sorting for parallel lithium-ion battery systems: Evaluation based on an electric circuit model," J. Energy Storage, vol. 6, pp. 195–203, May 2016.

[30] C. Pastor-Fernández, T. Bruen, W. D. Widanage, M. A. Gama-Valdez, and J. Marco, "A study of cell-to-cell interactions and degradation in parallel strings: implications for the battery management system," J. Power Sources, vol. 329, pp. 574–585, Oct. 2016.

[31] B. Kenney, K. Darcovich, D. D. MacNeil, and I. J. Davidson, "Modelling the impact of variations in electrode manufacturing on lithium-ion battery modules," J. Power Sources, Sep. 2012.

[32] R. Spurrett, C. Thwaite, A. Holland, D. Lizius, and G. J. Dudley, "Modeling of highly-parallel lithium-ion batteries," in Space Power, 2002, vol. 502, p. 685.

[33] R. Gogoana, M. B. Pinson, M. Z. Bazant, and S. E. Sarma, "Internal resistance matching for parallel-connected lithium-ion cells and impacts on battery pack cycle life," J. Power Sources, vol. 252, pp. 8–13, Apr. 2014